Scientific Research Publishing

Open Journal of Modern Hydrology, 2025, 15(2), 91-108
https://www.scirp.org/journal/ojmh
ISSN Online: 2163-0496
ISSN Print: 2163-0461

Investigation of the Hydraulic Conductivity of Fractures in a Limestone Rock Mass

Srđan Spasojević

Geo.tunnel.konsult LLC, Belgrade, Serbia
Email: srdjan.s@geotunnelkonsult.com

How to cite this paper: Spasojević, S. (2025) Investigation of the Hydraulic Conductivity of Fractures in a Limestone Rock Mass. *Open Journal of Modern Hydrology*, **15**, 91-108.
https://doi.org/10.4236/ojmh.2025.152007

Received: November 23, 2024
Accepted: March 2, 2025
Published: March 5, 2025

Abstract

In rock masses, water flows predominantly through the fractures, such as fissures and joints. Consequently, characterising the hydraulic conductivity of fractures is an essential parameter in the construction of dams and the design of grouting works or drainage systems. The hydraulic conductivity of low-permeability rock masses and fractures is commonly evaluated by water pressure tests (packer tests), which are typically performed for sections of several meters at a time. This study investigates the hydraulic conductivity of the fractures in the limestone foundation of Mratinje Dam. The new methods and knowledge evaluate the existing data recorded during the investigations in the past. Borehole packer test data are collected and examined from nine boreholes before the dam's construction. The results indicate that the Pareto and log-normal distributions can describe the fractures' hydraulic conductivity and apertures. The revealed hydraulic apertures explain why the grout curtain was not fully effective after the dam construction.

Keywords

Hydraulic Conductivity, Apertures, Water Pressure Tests, Limestones, Pareto, Log-Normal, Dams, Grouting Works

1. Introduction

Mratinje Dam is a concrete-arch-type dam located in the canyon of the Piva River in Montenegro, and it is the leading hydraulic structure in South-East Europe. The artificial lake "Piva" was formed behind the dam. The lake was formed by the diversion of the Piva River in 1975, by the construction of the dam, and by flooding part of the canyon. The dam is 220 m high and 261 m long, with a usable

volume of about 800 million cubic meters [1]. The dam is one of the highest in Europe and an exceptional construction success for the previous country, SFR Yugoslavia [2].

The massive geotechnical data, a rich bequest from the site where the dam is being constructed, including field tests, geology, fracture studies, rock quality designations, resistivity profiles, and water pressure tests (Lugeon), have been preserved. Some of these data are being re-examined to gain fresh perspectives and adopt an epistemophilic approach [2]-[4], a process that is essential for keeping our understanding of the dam site up to date.

Intriguing data records are water pressure tests performed during the investigation stages to determine the bedrock's permeability related to the grouting curtains' design. These data are processed and studied into important information in identifying how water flows through fractures and characterising the hydraulic conductivity of fractures and the rock mass at the dam site.

Hence, this research aims to investigate the spatial distribution of hydraulic conductivity with depth and its relationship to fracture intensity. The study's specific objectives were to calculate the equivalent hydraulic aperture and establish the distribution law of the equivalent hydraulic aperture, which is derived from statistical analysis.

These results are used to interpret the reported deficiencies in the grouting curtain in relation to the hydraulic aperture, the grouting penetration length, and the choice of grouting pressure and materials.

2. The Geology of the Study Site and Hydrological Conditions

The canyon at the dam's location is geomorphologically V-shaped, with very steep and nearly vertical valley sides. The entire left and right banks are made of massive Triassic limestone with an uneven distribution of fractures, **Figure 1**. According to their origin, the limestone is of the ridge type, influenced by significant tectonic movements in geological history.

The surfaces of the canyon are very uneven and gouged, which exclusively occurs on steep slopes related to thick layered and massive limestone, affected by the tectonic effects emphasized above, as well as by frost, precipitation, and insolation. As a result of all these processes but predominantly by mechanical weathering, larger dents were formed in many places at the base of the steep slopes. Dents were later filled by loose rock fragments and debris, accumulated each year and, conclusively, carved screes or talus slopes. Screes take the morphological forms of a sheet of debris and a talus cone.

The presence of several fractures in the limestone rock mass, as well as the carbonate composition, enabled the development of karstification. However, limestones have lower fracture density and low permeability near the dam. A smaller number of fractures and lower permeability indicate that they are shallower and less karstified at this place [4].

Groundwater location and regime are determined by the hydrogeological fea-

tures of the rock mass, as well as groundwater regime in the reservoir's hinterland and perception frequency. The level of the established aquifer fluctuates depending on changes in the water level in the reservoir of the dam. The groundwater level is similar to that in the reservoir, except in cases of infiltration from intense precipitation and after snow melting. This phenomenon is due to a tectonic fault in the hinterland that acts as a conductor and lowers the groundwater level. Once the water level in the reservoir is kept at the same level for a long time, a balance is established between the water level in the reservoir and the inflow of groundwater from the rock massif [5]

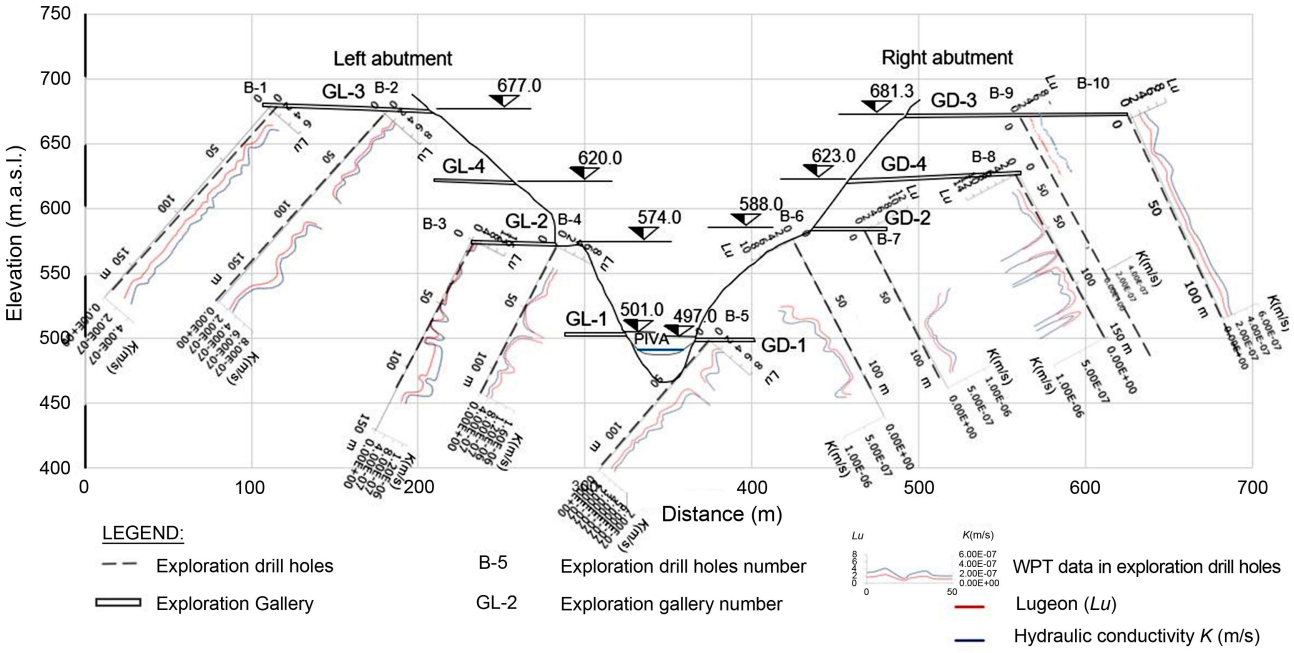

Figure 1. Cross-section, boreholes, and water pressure tests performed along the Mratinje Dam axis [4] [6].

3. Data Collection and Methods

3.1. Permeability Measurement Data in the Exploration Drill Holes

Water pressure or packer tests with the constant head are performed during the investigation stages to obtain the hydraulic parameters. The water pressure test is performed on isolated sections between expandable double packers. Water is inserted into the sealed test sections of five meters, and the water discharge (q) is measured. The water pressure (P) is applied in incremental stages up to its maximum value until the flow rate stops changing, and then the stages of relief of the water pressure till the end of the test. The flow is considered constant if the flow is measured during a few consecutive flow intervals of 5 min. However, sections with minor fractures and lower permeability take longer to reach a steady state. In this case, a steady state is considered if the difference between the two measurements is less than 10% of the measured flow. This indicates the flow has reached a quasi-steady state condition [7]. The tests were performed in boreholes drilled

to a depth of 120 to 180 m with a diameter of 76 mm. Detailed guidelines on the procedure for water pressure tests can be found in [8].

More than 100 tests of in-situ permeability of limestone rock were performed at the dam foundation. In the present study, only about 42 in-situ permeability tests are used to investigate the hydraulic conductivity of fractures in the dam foundation. Given that measurements have been performed for more than 50 years, only those measurements were selected that demonstrated stable flow, reached steady-state conditions, or where there was a measured number of fractures in the test sections. The permeability measurements are originally expressed in terms of the Lugeon value (Lu), which is empirically defined as the hydraulic conductivity required to achieve a flow rate of 1 liter/minute per meter of test interval under a reference water pressure equal to 1 MPa [9]:

$$Lu = \alpha \cdot \frac{q}{L} \cdot \frac{P_0}{P} \tag{1}$$

where α is a dimensionless factor and takes a value of $\alpha = 1$ in the international system of units (SI units). The water discharge (q) is determined by water take Q (Liters) and the injection time T(min), *i.e.*, $q = Q$(Liters)/T(min). The term P is the injection pressure used (MPa), and P_0 corresponds to a reference pressure equal to 1 MPa. The term L is the length of the isolated sections (m).

The hydraulic conductivity is expressed in terms of the m/s, accepting that the rock mass is homogeneous and isotropic and using a correlation between the Lugeon value (Lu) and hydraulic conductivity (K) of 1 $Lu = 1.3 \times 10^{-7}$ m/s [10].

3.2. Methodology of the Study

The hydraulic conductivity of fractures is governed by the aperture, length, and connectivity between the structures and by the conductivity effect of the fracture network, which can be partially open or closed [11].

The data collection comprised exploration drill holes and water pressure tests to investigate the hydraulic conductivity of fractures in the limestone rock mass. The primary dataset on geological structures is obtained from drill cores, which implies the classification of the rock mass, rock quality designation (RQD), and fracture counts. Unfortunately, measuring the geometry of fractures (strike and dip) was not viable since the drill cores were not oriented.

The key information on the hydraulic conductivity of fractures and rock mass explored in this study are as follows:

- The variation of the hydraulic conductivity related to the depth;
- The fracture intensity and relation to the hydraulic conductivity of fractures;
- Hydraulic aperture of fractures b_h.

3.2.1. The Variation of the Hydraulic Conductivity Related to the Depth

The hydraulic conductivity measurements in each borehole are used to create a histogram of log(K) values measured in section intervals. The log(K) data is analysed for any statistical dependence related to depth and to establish the statistical distribution of hydraulic conductivity of fractures with respect to depth.

3.2.2. Fracture Frequency and Relation to the Conductivity of Fractures

Information about the number of fractures from drill cores and the fracture intensity is important for rock mass permeability and water inflow estimation. A practical parameter for jointing the rock mass is lineal fracture intensity (P_{10}). The lineal fracture intensity (P_{10}) is a measure to account for the number of fractures per unit distance of drill hole length [12]. A change in P_{10} indicates a change in the rock masses, such as a fracture zone.

Similarly to the previous chapter, this data is combined with data from water pressure tests. The lineal fracture intensity (P_{10}) and the log(K) data are inspected for statistical dependence and setting of the statistical distribution of the hydraulic conductivity of fractures (K) related to the lineal fracture intensity (P_{10}).

3.2.3. Hydraulic Aperture of Fractures

Different distributions are fitted to the experimental distribution of section hydraulic conductivity, together with the number of fractures, to estimate the distribution of the fracture hydraulic apertures (b_h) along a borehole [13].

4. Results and discussion

4.1. Distribution of the Hydraulic Conductivity of Fractures by Depth

Studies have indicated that rock mass hydraulic conductivity regularly decreases systematically with depth [14]-[19]. The decrease in permeability with depth is usually attributed to the reduction of fracture aperture and fracture spacing with depth [20]. The decrease is due to higher in-situ stresses, lower fracture density, and degree of weathering and unloading.

The stress re-distribution appears in steep valleys, generating extensional fractures at shallow depths. To account for this effect, the relationship between the hydraulic conductivity (K) and the increase of depth (d_s) is examined. Here, the d_s is the shortest distance to the steep valley flanks.

Figure 2 shows that the hydraulic conductivity of the limestone does not exhibit a clear trend with depth, unlike crystalline rocks in Sweden [16] [18]. Besides, the median value of the hydraulic conductivity of the limestones is 1.9×10^{-7} m/s, while for crystalline rock is 7.9×10^{-8} m/s. This is 2.4 times higher compared to crystalline rocks. Nevertheless, the premise of the decrease in permeability with depth is accepted since the permeability of the karst aquifer is controlled by the degree of karst development. Therefore, the attenuation of karst development with depth can approximately represent the tendency for hydraulic conductivity to decay.

The variation of the hydraulic conductivity with the increase of depth (d_s) shows that it can be fitted by power-low distribution:

$$K = K_0 \cdot d_s^{-\beta} \tag{2}$$

where K_0 [m/s] is the hydraulic conductivity parameter, d_s [m] is the vertical depth from the valley flanks, and β is an exponent.

In this study, K_0 ranged from 1.50×10^{-6} m/s to 4.50×10^{-6} m/s, with the best fit at 2.45×10^{-6} m/s. The exponential parameter a is set to 0.55. The sample correlation (r) and coefficient of determination (R^2) between the K_{avg} and geometric mean of the hydraulic conductivity measurements is $r = 0.85$ and $R^2 = 0.72$, respectively. These are slightly lower but statistically significant values since this confirms that the above premise of the decrease in the hydraulic conductivity with depth is acceptable.

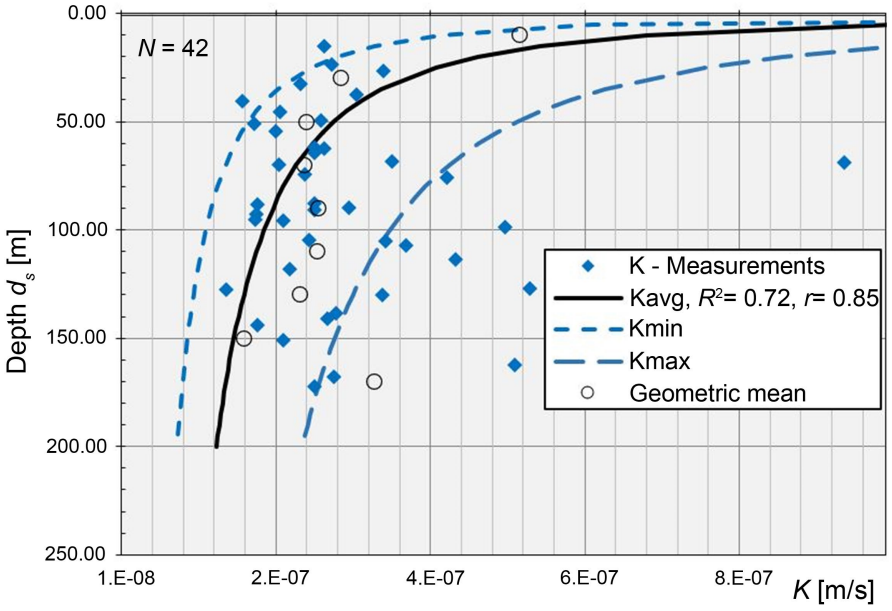

Figure 2. Variation of hydraulic conductivity of fractures by depth, interpreted from water pressure tests. The parameter N is the number of test data, R^2 is the coefficient of determination, and r is the sample correlation.

4.2. Hydraulic Conductivity Related to the Fracture Intensity

Collected data are processed to correlate the hydraulic conductivity to the lineal fracture intensity (P_{10}). Suppose the relatively large values of K with 0-1 fractures per meter and the lower values of K in the range of 3 - 4 fractures per meter are disregarded. In that case, the results show that the delineated values of the lineal fracture intensity (P_{10}) and hydraulic conductivity are consistent, *i.e.*, the sections of the borehole with a low value of fracture counts exhibited a lower permeability and vice versa.

The typical fracture intensity (P_{10}) data from the boreholes drilled in a limestone formation at a depth of 200 m are related to the hydraulic conductivity, as shown in Figure 3.

The variation of the hydraulic conductivity related to fracture intensity (P_{10}) can be fitted by power-low distribution:

$$K = a \cdot P_{10}^{b} \tag{3}$$

where a [m/s] is the hydraulic conductivity parameter, P_{10} [joints/m] is the

fracture intensity or number of fractures per unit meter of the borehole, and b is an exponent. In this study, a ranged from 1.3×10^{-7} m/s. The exponential parameter b is set to 1. The sample correlation (r) and coefficient of determination (R^2) between the fracture intensity (P_{10}) and the hydraulic conductivity measurements is $r = 0.46$ and $R^2 = 0.21$, respectively. If the relatively large and lower values of K are disregarded, as suggested above, the sample correlation (r) and coefficient of determination (R^2) rise to $r = 0.89$ and R^2=0.79, respectively.

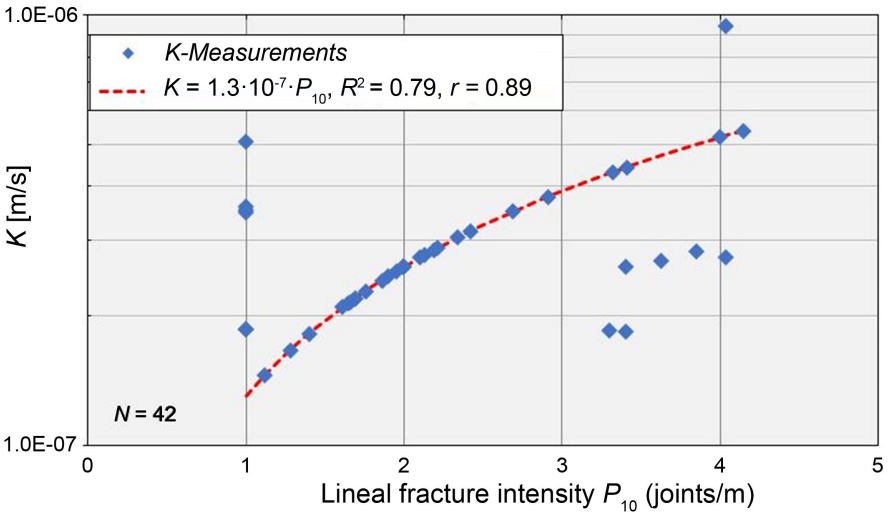

Figure 3. Hydraulic conductivity (K) variation related to fracture intensity (P_{10}). The parameter N is the number of test data, R^2 is the coefficient of determination, and r is the sample correlation.

4.3. Distribution of the Hydraulic Conductivity of Fractures

Various studies of rock mass verified that fracturing plays a decisive role in rock mass hydraulic conductivity. This is because water flow is concentrated in the fractures. Potential water flow paths are formed only in several fractures; therefore, only a few fractures are water-bearing and conductive.

The pivotal step in obtaining hydraulic parameters is assigning conductivity or transmissivity to the fracture network. Statistical methods are a typical tool employed to study the spatial variability of the hydraulic conductivity of fractures. These methods provide a probabilistic description of all individual fractures based on the input data. Numerous studies have consistently shown that the hydraulic conductivity of fractures typically follows a log-normal [21] [22] or bimodal/multimodal distribution [23] [24]. The log-normal distribution, the most widely used, is suitable for both homogeneous and heterogeneous rocks. Other distributions, such as the Levy stable distribution [25], are also viable options.

The simple power-low distribution, Pareto distribution [26], is exploited to correlate the hydraulic conductivity of individual fractures. By using this distribution, we can confidently assess the hydraulic conductivity based on a maxi-

mum hydraulic conductivity (K_{max}), estimated for the most conductive fracture in the tested sections [13]. This power-low distribution is verified to be reliable in cases where there are many thin fractures and only a few wide ones, *i.e.*, when the largest fracture controls the water inflow and, thereby, the hydraulic conductivity.

Using the Pareto distribution, the probability that the hydraulic conductivity (K) is lower than the section hydraulic conductivity (K_n) is calculated, $P(K < K_n)$, *i.e.*, a cumulative distribution function (*CDF*):

$$P(K_n) = P(K < K_n) = 1 - \left(\frac{K_{max}/K_n}{N+1} \right)^k \quad (4)$$

where n is the number of hydraulic conductivities in the sections, N is the total number of fractures, and K_{max} is the hydraulic conductivity of the largest fracture. In the case of the log-normal distribution [27], the probability that the hydraulic conductivity, K, is lower than the section hydraulic conductivity (K_n) is calculated according to the cumulative distribution function (*CDF*) of the log-normal distribution:

$$P(K_n) = P(K < K_n) = \Phi\left(\frac{\ln K}{\sigma} \right) = \frac{1}{2}\left[1 + erf\left(\frac{\ln K - \mu}{\sqrt{2} \cdot \sigma} \right) \right] \quad (5)$$

where Φ is the cumulative distribution function of the normal distribution, μ and σ are the mean and standard deviation of the natural logarithm of the fracture aperture, respectively.

The hydraulic conductivity for both distributions combined for all fractures is plotted on the semi-logarithmic histogram in **Figure 4**. The collected test data illustrated that the hydraulic conductivity values range over one order of magnitude from 10^{-7} to 10^{-6} m/s, *i.e.*, between 1.3×10^{-7} m/s and 5.4×10^{-7} m/s. Isolated discontinuities may have hydraulic conductivity of 5.20×10^{-7} to 9.46×10^{-7} m/s.

Both distribution curves, the power low (Pareto) and log-normal, can be fitted to the hydraulic conductivity measurements in **Figure 4**. They fit well with the geometric means of the variation of K for the depths of 40 m to 140 m. The geometric mean of K is calculated at every 20 m interval [28]-[31]. Several discrepancies are observed for the shallow depths (<40 m) and depths more than 140 m.

The Pareto distribution fitting gives a straight line in a log-log plot [32]; see **Figure 5**. Approximation gives a slope ($-k$) value of 0.955, whereas the K_{max} is 9.46 $\times 10^{-7}$ m/s. The sample correlation (r) and coefficient of determination (R^2) between the measurements of K and Pareto estimates of K are $r = 0.22$ and $R^2 = 0.05$, respectively.

In the case of the log-transformed K data ($\ln K$), a geometric mean (K_g) is 2.6×10^{-7} m/s and a standard deviation ($\sigma_{\ln K}$) of 0.40 for the log-transformed K data ($\ln K$). The sample correlation (r) and the coefficient of determination (R^2) between the measurements of K and log-transformed data ($\ln K$) are $r = 0.33$ and $R^2 = 0.11$, respectively.

For both distribution fittings, the sample correlation (r) and the coefficient of

determination R^2 are small but statistically significantly correlated. The p-values for the Pareto distribution and log-normal are $p = 0.016$ and $p = 0.029$, respectively, and are less than the significance level ($p \leq 0.05$) [33].

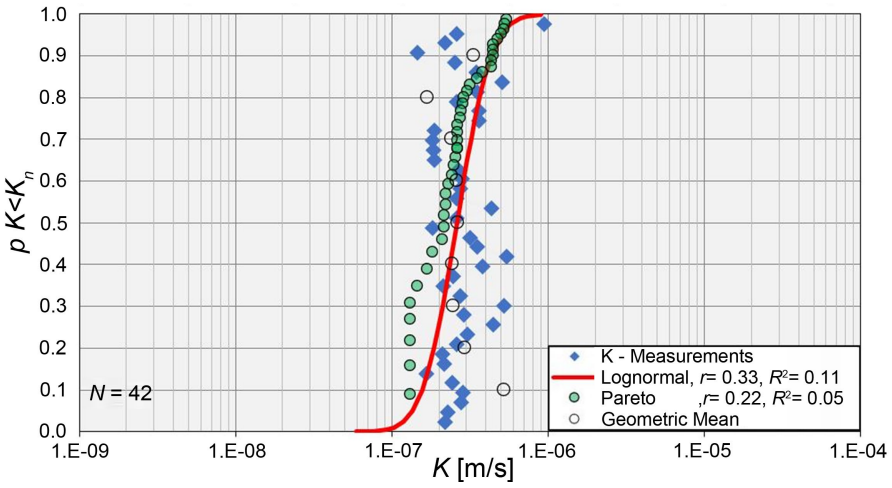

Figure 4. Cumulative distribution plots of hydraulic conductivity data at the Mratinje Dam and the corresponding Pareto and Log-normal distributions.

4.4. Hydraulic Conductivity Related to Fracture Aperture

Hydraulic conductivity is a parameter expressing the flow through the joint under the influence of frictional losses, tortuosity, and channeling [34]. The hydraulic conductivity of fractured rock masses is generally strongly heterogeneous and ranges over several orders of magnitude. Many factors influence the hydraulic conductivity of fractures in the rock, including fracture orientation, density, connectivity, and apertures [35]-[38].

All these factors significantly affect the flow; however, laminar and viscous flow is often approximated to stationary, incompressible single flow between smooth parallel plates where fluid is chemically inert to the rock medium. In such cases, the hydraulic conductivity of a single fracture is obtained by solving the Navier-Stokes equation [39], which leads to the cubic law [14] [40] [41].

Under the cubic law terms, the fracture hydraulic conductivity (K) is dependent on the fracture aperture, b_h, and may be written as:

$$K = \frac{\rho_w g}{\mu_w} \frac{b_h^3}{12} \tag{6}$$

where g is gravity acceleration, b_h is the hydraulic aperture, μ_w, and ρ_w are the kinematic viscosity and density of water, respectively.

The cubic law expresses an "open" channel flow condition, *i.e.*, a volumetric flow rate (permeability) through the fractures is completely dependent and linearly proportional to their aperture. Fracture surfaces remain parallel and are not in contact at any point, and a constant hydraulic aperture and a constant hydraulic conductivity of fractures are assumed.

In reality, fractures have variable apertures and contact areas. The simplifica-

tion of smooth parallel plates produces the smallest errors for large aperture fractures. The assumption that the largest fracture dominates the flow is supported by the cubic law.

The number of fractures along isolated sections is combined with the hydraulic conductivity data from water pressure tests to estimate the hydraulic fracture aperture distribution. This process uses hydraulic conductivity (K) to express the amount of water that can be transported through a fracture.

This study uses a power-law, Pareto distribution, to fit the hydraulic aperture distribution identically as the hydraulic conductivities (K) was done previously. The hydraulic apertures follow the Pareto distribution with the parameter $3k$. For an interpretation of how the cubic law is coupled with the Pareto distribution, we refer to [13]. A plot of fracture hydraulic conductivities evaluated by the nonparametric method is shown in Figure 5.

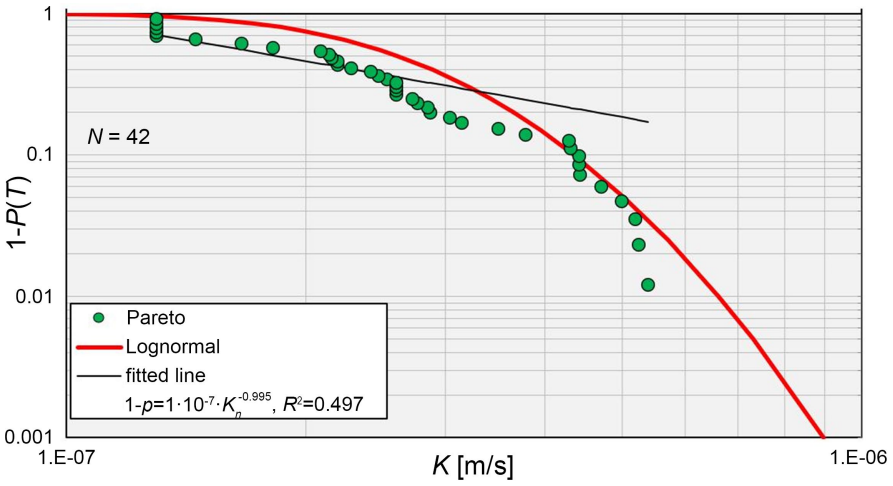

Figure 5. A derived distribution curve fitted to the measured values of hydraulic conductivities.

Subsequently, the cubic law is re-arranged so that the hydraulic aperture (b_h) is related to the hydraulic conductivity (K). This way, hydraulic aperture distribution can be estimated. The procedure involves the use of the slope parameter (k) maximum estimated hydraulic aperture ($b_{\max}$) and the rank (r) by the following equitation:

$$b_r = \frac{b_{\max}}{r^{\frac{1}{3k}}} \tag{7}$$

$$b_{\max} = \sqrt[3]{K_{\max} \cdot L \cdot \frac{12\mu}{\rho g}} \tag{8}$$

where L is an isolated section length, and $K_{\max}$ is the maximal hydraulic conductivity of the hydraulic aperture.

Figure 6 presents simulated fracture apertures from the datasets and reflects the relative content of different hydraulic apertures of the rock mass. The simulation uses Pareto properties to represent the total flow related to the number of fractures.

The maximum hydraulic aperture, b_{max} = 195.87 μm, is estimated using the maximum hydraulic conductivity value obtained previously, K_{max} = 9.46·10^{-7} m^2/s. The log-normal simulation is approximated with a geometric mean (b_g) of 58.29 μm and a standard deviation ($\sigma_{\ln b}$) of 0.40 for the log-transformed b_h data ($\ln b_h$).

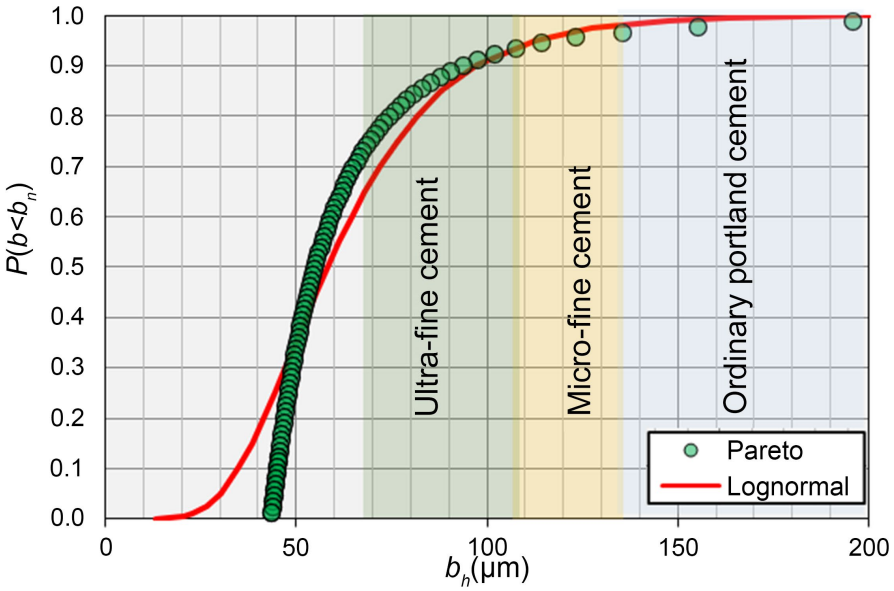

Figure 6. Cumulative plot of simulated fracture hydraulic apertures.

Calculated hydraulic apertures from the Pareto distribution range from 50 μm to 200 μm and that within this range, 90% of the fractures have smaller hydraulic apertures than 93.28 μm and 10% have smaller hydraulic apertures than 45.12 μm.

Calculated hydraulic apertures from the Log-normal distribution range from 20 μm to 200 μm, and within this range, 90% of the fractures have smaller hydraulic apertures than 97.33 μm, and 10% have smaller hydraulic apertures than 34.91 μm.

Revealed hydraulic apertures of fractures could explain why the grouting curtain of the dam has not reached the required sealing effects. Initially, the three-row grout curtain is constructed from the access tunnels to seal off the dam foundation. After 1976, a few additional repair measures of the grout curtains were performed. Nevertheless, additional measurements and tests during 2009 indicated that the efficient functionality of the curtain has not yet been reached [5].

The grouting methodology used for the construction and later for repairing the grouting curtain was not adequate. The grouting was performed by applying the downward method with low grouting pressures up to 0.5 - 0.6 MPa. The grouting is performed in sections of 5 m with 3 m intervals of boreholes. The higher grouting pressures were more suitable, although the applied grouting agent is more problematic.

The grouting agent used was Portland cement with a w/c ratio of 4:1 and the addition of 5% bentonite. Such grouting material is not able to seal fractures with

hydraulic apertures, as shown in Figure 6. Hence, many fractures with smaller apertures remained unsealed, allowing water to drip and making the grouting curtain inefficient.

Hydraulic apertures identified in this study and recent research on grouting materials suggest that various types of cement, particularly those with a grain size of d_{95} down to 16 μm and a viscosity ranging from 10 to approximately 50 mPa s, are required for full joint penetrability and effective filtration mitigation. This is essential for achieving successful grouting results and ensuring proper retrofitting of dam foundations.

5. Conclusions

In this study, 42 hydraulic conductivity measurements were collected by water pressure tests from 9 boreholes at the location of a 220 m high dam in Montenegro.

Although larger sample sizes provide stronger and more reliable results, this data sample size is sufficient to make a statistically reliable conclusion about a population. Especially being mindful that this study has been performed on data collected more than 50 years before.

The field results indicate that the limestone rock mass has a conductivity between 1.3×10^{-7} and 5.4×10^{-7} m/s at a depth up to 200 m below the ground surface. In general, the average rock mass conductivity is 3.02×10^{-7} m/s. Isolated discontinuity zones may flows through discontinuity networks underground and have a conductivity of 5.20×10^{-7} to 9.46×10^{-7} m/s.

The results indicate that the general trend of hydraulic conductivity decreases with depth, similar to the observations by other researchers, and can be fitted by power-low distribution. The coefficient of determination for the power-law fit is comparable to that of crystalline rocks.

The variation of the hydraulic conductivity related to fracture intensity (P_{10}) can also be fitted by power-low distribution. If the relatively large and lower values of K are disregarded, the coefficient of determination is very strong. However, further work is required because the power-law distribution demonstrates a moderately strong relationship when all data are considered.

An analysis of field data from boreholes has shown that a power-law and log-normal distribution could describe the hydraulic conductivity related to individual fractures. For both distribution fittings, the sample correlation (r) and the coefficient of determination R^2 are small but statistically significantly correlated.

The equivalent hydraulic aperture of fractures is calculated based on cubic law, and the statistical distribution law of the equivalent hydraulic aperture is obtained based on a power-law and log-normal distribution. There is no obvious indication that power law distribution fits the data better than a lognormal, as suggested in [42]. The calculated hydraulic apertures range from 20 μm to 200 μm and within this range, 90% of the fractures have smaller hydraulic apertures than 90 - 100 μm and 10% have smaller hydraulic apertures than 35 - 45 μm.

Observations of the water seepage flow during 2009 indicated that the grout curtain was not fully effective. Insight into the content of different hydraulic apertures reveals that one reason is that the grouting agent employed is not inadequate. It is believed that the applied type of grout (Portland cement and w/c ratio) had limited penetration length and could not entirely seal fractures with smaller apertures. This finding aligns with the grouting practice, which is evidenced that ordinary cement-based grouts penetrate fractures with a hydraulic aperture down to 100 - 150 μm. If fractures with a smaller hydraulic aperture are to be sealed, cement grouts with fine-grain or non-cementitious grouts may be required. The grouting could be operated with more suitable grouting pressures.

The reported deficiencies are explicable considering the time of the dam construction and the availability of technology at that point, keeping in mind that we stare at the past through the eyes of the present knowledge. The grouting technology has developed considerably over the last 20 years. Nowadays, the selection of appropriate grout material depends on the size, frequency, and configuration of the fractures in the rock mass. The particle size of the grout material also plays a key role in the selection criteria of grout.

Data Availability

The data used and/or analysed during the current study will be made available from the corresponding author on reasonable request.

Conflicts of Interest

The author wishes to confirm that there are no known conflicts of interest associated with this publication, and there has been no significant financial support for this work that could have influenced its outcome.

References

[1] Spasojević, S. (2022) Single-Layer Load-Bearing Tunnel Lining Structure in Hard Rock Masses. *Gradjevinski materijali i konstrukcije*, **65**, 167-177. https://doi.org/10.5937/grmk2204167s

[2] Ivanović, K., Jovanović, L., Kujundzić, B., Marković, O., Radosavljevic, Ž., Tričković, T. and Petrović, P. (1974) The Results of Testing the Mechanical Characteristics of the Rock Mass in the Foundations of the Mratinje Dam. *Symposium on the construction of HPP Mratinje*, Nikšić, 24-26 May 1974, 65-76.

[3] Ivanovíć, K., Jovanovíć, L., Marković, O. and Kujundzić, B. (1970) Complex Research of Rock Mass Mechanical Characteristics for the Mratinje Arch Dam. *Proceeding of 2nd ISRM Congress*, Belgrade, 21 September 1970.

[4] Jovanović, L., Kujundzić, B., Marković, O., Radosavljević, Ž. and Božović, A. (1972) HPP "Mratinje" Detailed Design—Geology. Energoprojekt.

[5] Belićević, V. and Knežević, D. (2011) Antifiltration Grout Curtain of Hydropower Plant Piva—Mratinje Dam. In: Mir, M.A., Garcia, R.R., *et al.*, Eds., *Dam Maintenance and Rehabilitation*, Taylor and Francis, 415-425.

[6] Kujundzić, B. (1979) Use of Tests and Monitoring in the Design and Construction of

Rock Structures. *Proceeding of* 4*th International Congress Rock Mechanics* (*ISRM*), Montreux, September 1979, 181-186.

[7] Butron, C. (2012) Drip Sealing Grouting of Tunnels in Crystalline Rock: Conceptualization and Technical Strategies. Ph.D. Thesis, Chalmers University of Technology.

[8] Vaskou, P., de Quadros, E.F., Kanji, M.A., Johnson, T. and Ekmekci, M. (2019) ISRM Suggested Method for the Lugeon Test. *Rock Mechanics and Rock Engineering*, **52**, 4155-4174. https://doi.org/10.1007/s00603-019-01954-x

[9] Quiñones-Rozo, C. (2010) Lugeon Test Interpretation, Revisited. Collaborative Management of Integrated Watersheds, Bliss, 405-414

[10] Fell, R., MacGregor, P., Stapledon, D. and Bell, G. (2005) Geotechnical Engineering of Dams. Taylor & Francis. https://doi.org/10.1201/NOE0415364409

[11] Laubach, S.E., Lander, R.H., Criscenti, L.J., Anovitz, L.M., Urai, J.L., Pollyea, R.M., *et al*. (2019) The Role of Chemistry in Fracture Pattern Development and Opportunities to Advance Interpretations of Geological Materials. *Reviews of Geophysics*, **57**, 1065-1111. https://doi.org/10.1029/2019rg000671

[12] Dershowitz, W.S. and Herda, H.H. (1992) Interpretation of Fracture Spacing and Intensity: Dershowitz, W S; Herda, H H Proc 33rd US Symposium on Rock Mechanics, Santa Fe, 3-5 June 1992 P757-766. Publ Rotterdam: A A Balkema, 1992. *International Journal of Rock Mechanics and Mining Sciences & Geomechanics Abstracts*, **30**, A212. https://doi.org/10.1016/0148-9062(93)91769-f

[13] Gustafson, G. and Fransson, Å. (2005) The Use of the Pareto Distribution for Fracture Transmissivity Assessment. *Hydrogeology Journal*, **14**, 15-20. https://doi.org/10.1007/s10040-005-0440-y

[14] Snow, D.T. (1969) Anisotropie Permeability of Fractured Media. *Water Resources Research*, **5**, 1273-1289. https://doi.org/10.1029/wr005i006p01273

[15] Louis, C. (1974) Rock Hydraulics in Rock Mechanics. Springer Verlag.

[16] Carlsson, A. and Olsson, T. (1977) Hydraulic Properties of Swedish Crystalline Rocks-Hydraulic Conductivity and Its Relation to Depth. Bulletin of the Geological Institute, 71-84.

[17] Burgess, A. (1977) Groundwater Movements around a Repository Regional Groundwater Analysis. Kaernbraenslesaekerhet.

[18] Black, H.J. (1987) Flow and Flow Mechanisms in Crystalline Rock. In: *The Geology of Fluid Flow*: *Fluid Flow in Sedimentary Basins and Aquifers*, Blackwell Scientific, 185-200. https://doi.org/10.1144/GSL.SP.1987.034.01.13

[19] Wei, Z.Q., Egger, P. and Descoeudres, F. (1995) Permeability Predictions for Jointed Rock Masses. *International Journal of Rock Mechanics and Mining Sciences & Geomechanics Abstracts*, **32**, 251-261. https://doi.org/10.1016/0148-9062(94)00034-z

[20] Lakshmanan, E. (2011) Hydraulic Conductivity—Issues, Determination and Applications. IntechOpen, https://doi.org/10.5772/744

[21] Woodbury, A.D. and Sudicky, E.A. (1991) The Geostatistical Characteristics of the Borden Aquifer. *Water Resources Research*, **27**, 533-546. https://doi.org/10.1029/90wr02545

[22] Rehfeldt, K.R., Boggs, J.M. and Gelhar, L.W. (1992) Field Study of Dispersion in a Heterogeneous Aquifer: 3. Geostatistical Analysis of Hydraulic Conductivity. *Water Resources Research*, **28**, 3309-3324. https://doi.org/10.1029/92wr01758

[23] Freeze, R.A. (1975) A Stochastic-Conceptual Analysis of One-Dimensional Groundwater Flow in Nonuniform Homogeneous Media. *Water Resources Research*, **11**,

725-741. https://doi.org/10.1029/wr011i005p00725

[24] Genereux, D.P., Leahy, S., Mitasova, H., Kennedy, C.D. and Corbett, D.R. (2008) Spatial and Temporal Variability of Streambed Hydraulic Conductivity in West Bear Creek, North Carolina, USA. *Journal of Hydrology*, **358**, 332-353. https://doi.org/10.1016/j.jhydrol.2008.06.017

[25] Lu, C., Qin, W., Zhao, G., Zhang, Y. and Wang, W. (2017) Better-Fitted Probability of Hydraulic Conductivity for a Silty Clay Site and Its Effects on Solute Transport. *Water*, **9**, Article 466. https://doi.org/10.3390/w9070466

[26] Arnold, C. (1983) Pareto Distributions, MD. International Co-Operative Publishing House.

[27] Aitchison, J. and Brown, A.J. (1957) The Lognormal Distribution. Cambridge University Press.

[28] Warren, J.E. and Price, H.S. (1961) Flow in Heterogeneous Porous Media. *Society of Petroleum Engineers Journal*, **1**, 153-169. https://doi.org/10.2118/1579-g

[29] Desbarats, A.J. (1987) Numerical Estimation of Effective Permeability in Sand-shale Formations. *Water Resources Research*, **23**, 273-286. https://doi.org/10.1029/wr023i002p00273

[30] Durlofsky, L.J. (1991) Numerical Calculation of Equivalent Grid Block Permeability Tensors for Heterogeneous Porous Media. *Water Resources Research*, **27**, 699-708. https://doi.org/10.1029/91wr00107

[31] Hinrichsen, E.L., Aharony, A., Feder, J., Hansen, A., Jøssang, T. and Hardy, H.H. (1993) A Fast Algorithm for Estimating Large-Scale Permeabilities of Correlated Anisotropic Media. *Transport in Porous Media*, **12**, 55-72. https://doi.org/10.1007/bf00616362

[32] Zipf, K. (1949) Human Behavior and the Principle of Least Effort: An Introduction to Human Ecology. Addison-Wesley Press.

[33] Forbes, C., Evans, M., Hastings, N. and Peacock, B. (2010) Statistical Distributions. 4th Edition, Wiley. https://doi.org/10.1002/9780470627242

[34] Priest, S. (1973) Discontinuity Analysis for Rock Engineering. Chapman & Hall. https://doi.org/10.1007/978-94-011-1498-1

[35] Norton, D. and Knapp, R. (1977) Transport Phenomena in Hydrothermal Systems; the Nature of Porosity. *American Journal of Science*, **277**, 913-936. https://doi.org/10.2475/ajs.277.8.913

[36] Sausse, J. (1998) Caractérisation et modélisation des écoulements fluides en milieu fissuré. Relation avec les altérations hydrothermales et quantification des paléocontraintes. Université Henri Poincaré-Nancy. https://theses.hal.science/tel-00011716v2

[37] Stober, I. and Bucher, K. (2007) Hydraulic Properties of the Crystalline Basement. *Hydrogeology Journal*, **15**, 1643-1643. https://doi.org/10.1007/s10040-007-0214-9

[38] Laubach, S.E., Lamarche, J., Gauthier, B.D.M., Dunne, W.M. and Sanderson, D.J. (2018) Spatial Arrangement of Faults and Opening-Mode Fractures. *Journal of Structural Geology*, **108**, 2-15. https://doi.org/10.1016/j.jsg.2017.08.008

[39] Galdi, G.P. (2012) Navier-Stokes Equations: A Mathematical Analysis. In: Meyers, R., Ed., *Mathematics of Complexity and Dynamical Systems*, Springer, 1009-1042. https://doi.org/10.1007/978-1-4614-1806-1_60

[40] Witherspoon, P.A., Wang, J.S.Y., Iwai, K. and Gale, J.E. (1980) Validity of Cubic Law for Fluid Flow in a Deformable Rock Fracture. *Water Resources Research*, **16**, 1016-1024. https://doi.org/10.1029/wr016i006p01016

[41] Milsch, H., Hofmann, H. and Blöcher, G. (2016) An Experimental and Numerical Evaluation of Continuous Fracture Permeability Measurements during Effective Pressure Cycles. *International Journal of Rock Mechanics and Mining Sciences*, **89**, 109-115. https://doi.org/10.1016/j.ijrmms.2016.09.002

[42] Santos, R.F.V.C., Miranda, T.S., Barbosa, J.A., Gomes, I.F., Matos, G.C., Gale, J.F.W., *et al*. (2015) Characterization of Natural Fracture Systems: Analysis of Uncertainty Effects in Linear Scanline Results. *AAPG Bulletin*, **99**, 2203-2219. https://doi.org/10.1306/05211514104

Nomenclature

a	hydraulic conductivity parameter (m/s)
b	fitting exponent parameter (−)
b_h	the hydraulic aperture of fracture (m)
$b_{\max}$	the maximum estimated hydraulic aperture of fracture (m)
b_r	the hydraulic aperture of the fracture with rank r (m)
b_n	the hydraulic aperture of fractures in the section (m)
b_g	the geometric mean of the log-transformed b_h data (m)
CDF	cumulative distribution function (−)
d_{95}	the particle size value at which the cumulative distribution percentage from smallest to largest reaches 95% in the particle size distribution
d_s	the vertical depth from the valley flanks (m)
erf	Gauss error function (−)
Φ	the cumulative distribution the function of the normal distribution (−)
g	gravity acceleration (m/s^2)
K	the hydraulic conductivity (m/s)
K_0	hydraulic conductivity parameter (m/s)
K_{avg}	the average hydraulic conductivity (m/s)
$K_{\min}$	the hydraulic conductivity of the smallest fracture (m/s)
$K_{\max}$	the hydraulic conductivity of the largest fracture (m/s)
K_n	the section hydraulic conductivity (m/s)
K_g	the geometric mean of the log-transformed K data (m/s)
k	the Pareto slope parameter (−)
L	isolated section length (m)
Lu	Lugeon value (−)
n	number of hydraulic conductivities in the section (−)
N	the total number of fractures (−)
P	the water injection pressure (MPa)
P_0	reference pressure (equal to 1 MPa)
P_{10}	lineal fracture intensity (−)
q	the water discharge during water pressure tests (L/min)
Q	the water taken (flow rate) during water pressure tests (L)
r	sample correlation (−)
$r(rank)$	the rank of a measured value in an ordered sample (−)
R^2	coefficient of determination (−)
RQD	rock quality designation (−)
T	the water injection time (min)

α	the dimensionless factor for Lu conversion in SI international system) or IS (imperial measures)
β	fitting exponent parameter (–)
μ	the mean of the natural logarithm (ln m/s)
μ_w	the kinematic viscosity of water (Pa·s)
ρ_w	density of water (kg/m^3)
σ	the standard deviation of the natural logarithm (–)
$\sigma_{\ln K}$	the standard deviation for the log-transformed K data (–)
$\sigma_{\ln b}$	the standard deviation for the log-transformed b_h data (–)